# $Zn^{2+}$ Modulation of Neuronal Transient $K^+$ Current: Fast and Selective Binding to the Deactivated Channels

Chung-Chin Kuo and Fang-Ping Chen
Department of Physiology, National Taiwan University College of Medicine, and Department of Neurology, National Taiwan University Hospital, Taipei 100, Taiwan, Republic of China

ABSTRACT Modulation of voltage-dependent transient $K^+$ currents (A type $K^+$ or $K_A$ current) by $Zn^{2+}$ was studied in rat hippocampal neurons by the whole-cell patch-clamp technique. It is found that $Zn^{2+}$ selectively binds to the resting (deactivated or closed) $K_A$ channels with a dissociation constant ($K_d$) of ~3 $\mu$M, whereas the affinity between $Zn^{2+}$ and the inactivated $K_A$ channels is 1000-fold lower. $Zn^{2+}$ therefore produces a concentration-dependent shift of the $K_A$ channel inactivation curve and enhances the $K_A$ current elicited from relatively positive holding potentials. It is also found that the kinetics of $Zn^{2+}$ action are fast enough to compete with the transition rates between different gating states of the channel. The rapid and selective binding of $Zn^{2+}$ to the closed $K_A$ channels keeps the channel in the closed state and explains the ion's concentration-dependent slowing effect on the activation of $K_A$ current. This in turn accounts for the inhibitory effect of $Zn^{2+}$ on the $K_A$ current elicited from hyperpolarized holding potentials. Because the molecular mechanisms underlying these gating changes are kinetic interactions between the binding-unbinding of $Zn^{2+}$ and the intrinsic gating processes of the channel, the shift of the inactivation curve and slowing of $K_A$ channel activation are quantitatively correlated with ambient $Zn^{2+}$ over a wide concentration range without "saturation"; i.e., The effects are already manifest in micromolar $Zn^{2+}$, yet are not saturated even in millimolar $Zn^{2+}$. Because the physiological concentration of $Zn^{2+}$ could vary over a similarly wide range according to neural activities, $Zn^{2+}$ may be a faithful physiological "fine tuner," controlling and controlled by neural activities through its effect on the $K_A$ current.

## INTRODUCTION

Transient $K^+$ current is widely present in neurons and plays an important role in regulating discharge patterns of the cell (for a review see Hille, 1992). $Zn^{2+}$ is a transitional metal ion present in the central nervous system (Gooddy et al., 1974; Palm and Hallmans, 1982) and is especially enriched in areas such as the hippocampal formation (Frederickson et al., 1983; Slomianka, 1992). It has been shown that $Zn^{2+}$ has two different effects on neuronal $K_A$ current. When $K_A$ current is elicited by a step depolarization from negative holding potentials, the peak current is inhibited by $Zn^{2+}$. On the other hand, when the holding potential is more positive, $Zn^{2+}$ enhances the $K_A$ current (Harrison et al., 1993; Huang et al., 1993; Bardoni and Belluzzi, 1994; see also Fig. 1, *A* and *B*). The dual effects may be ascribable to the modulation of $K_A$ channel gating by $Zn^{2+}$. $Zn^{2+}$ shifts the steady-state inactivation curve of $K_A$ current toward more depolarized potentials (Harrison et al., 1993; Huang et al., 1993; Bardoni and Belluzzi, 1994; Talukder and Harrison, 1995) and slows activation as well as lengthens the time to peak of $K_A$ current (Harrison et al., 1993; Bardoni and Belluzzi, 1994; Spires and Begenisich, 1994). Shift of the inactivation curve readily explains $Zn^{2+}$ enhancement of $K_A$ current elicited from positive holding potentials. With an unchanged inactivation rate (Bardoni and Belluzzi, 1994), the slowed activation could account for the inhibition of peak $K_A$ current elicited from negative holding potentials by $Zn^{2+}$.

Although the effects of $Zn^{2+}$ on $K_A$ current are ascribable to changes in channel gating, the molecular mechanisms underlying such gating changes have not been fully characterized. One way to envisage the molecular action of $Zn^{2+}$ is the modal gating hypothesis, which is originally proposed for the action of dihydropyridine drugs on L-type $Ca^{2+}$ channels by Hess and Tsien (1984). According to this hypothesis, $Zn^{2+}$-bound $K_A$ channels would be in a new gating mode and are activated more slowly and require more positive potential to be inactivated (Fig. 1 *C*). Based on the modal gating hypothesis, Harrison et al. (1993) and Davidson and Kehl (1995) fitted a Hill equation to the concentration-dependent shift of the inactivation curve by $Zn^{2+}$ and estimated the dissociation constant ($K_d$) between $Zn^{2+}$ and $K_A$ channels to be 14–93 $\mu$M. Spires and Begenisich (1994) also measured the affinity between $Zn^{2+}$ and the $K_A$ channel with similar rationales. However, the modal gating hypothesis requires that the kinetics of $Zn^{2+}$ binding-unbinding be much slower than the transition rates between different intrinsic gating states of the channel, and there has been no attempt to determine whether such a fundamental presumption is valid. Moreover, the prominent shift of the steady-state inactivation curve indicates that $Zn^{2+}$ has a very different affinity for different gating states (e.g., the resting and the inactivated states) of the $K_A$ channel, but so far previous studies reported only a single $K_d$ without specifying the $K_d$ to a gating state of the channel. We therefore

*Received for publication 27 May 1999 and in final form 10 August 1999.*
Address reprint requests to Dr. Chung-Chin Kuo, Department of Physiology, National Taiwan University College of Medicine, No. 1, Jen-Ai Rd., 1st Section, Taipei 100, Taiwan, Republic of China. Tel: 886-2-23123456, ext. 8236; Fax: 886-2-23964350; E-mail: cckuo@ha.mc.ntu.edu.tw.

0006-3495/99/11/2552/11 $2.00

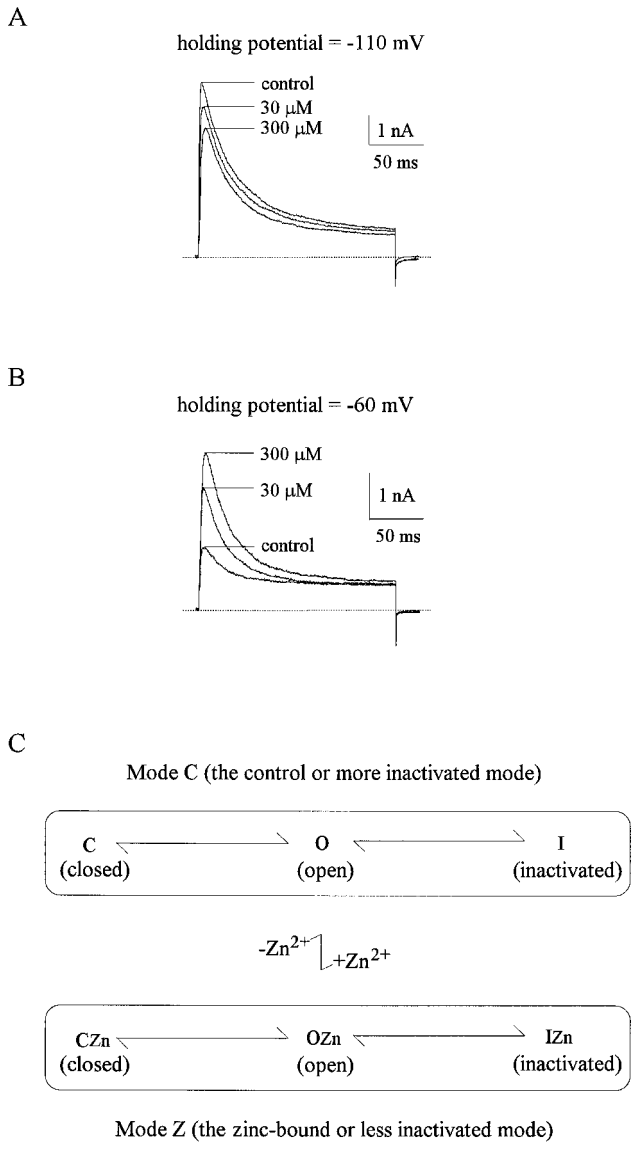


FIGURE 1 The effect of $Zn^{2+}$ on $K_A$ current and the modal gating hypothesis. (*A*) $Zn^{2+}$ inhibits $K_A$ current elicited from negative holding potentials. The cell was held at −110 mV and stepped every 2 s to +50 mV for 200 ms to elicit $K_A$ current, which is inhibited by 30–300 $\mu$M $Zn^{2+}$. The dashed line denotes zero current level. (*B*) $Zn^{2+}$ enhances $K_A$ current elicited from relatively positive holding potentials. The same cell and the same pulse protocol as those in *A*, except that the cell was held at −60 mV rather than −110 mV. $Zn^{2+}$ (30–300 $\mu$M) now enhances rather than inhibits the transient current. The dashed line denotes zero current level. (*C*) The model gating hypothesis explaining $Zn^{2+}$ action. The $K_A$ channels normally gate in mode C. However, the channel would gate differently in mode Z when $Zn^{2+}$ is bound to the channel. At any particular membrane potential, the channel in mode Z activates more slowly and is inactivated less readily than the channel in mode C. The kinetics of $Zn^{2+}$ action presumably are so much slower than the intrinsic gating process (a fundamental assumption of the hypothesis) that one may disregard changes between the $Zn^{2+}$-free and the $Zn^{2+}$-bound channels while discussing changes between the resting channels and the inactivated channels. Kinetic interactions between $Zn^{2+}$ binding-unbinding and gating transitions are thus disregarded, and the binding and unbinding of $Zn^{2+}$ to and from discrete gating states of $K_A$ channels are not individually considered. $Zn^{2+}$ is simplified to a modulator controlling the relative proportions of modes C and Z.

study $Zn^{2+}$ action on central neuronal $K_A$ current in more detail and find that $Zn^{2+}$ has a much higher affinity for the resting $K_A$ channel (dissociation constant ~3 $\mu$M) than for the inactivated $K_A$ channel. It is also found that the kinetics of $Zn^{2+}$ action are not slow enough to justify the modal gating hypothesis. Instead, the slowed activation is probably due to fast and selective binding of $Zn^{2+}$ to the deactivated channel, which tends to keep the channel in the resting state and thus deters its activation.

## MATERIALS AND METHODS

### Cell preparation

Coronal slices of the whole brain were prepared from 7–14-day-old Long-Evans rats. The CA1 region was dissected from the slices and cut into small chunks. After treatment for 5–10 min at 37°C in dissociation medium (in mM, 82 $Na_2SO_4$, 30 $K_2SO_4$, 3 $MgCl_2$, 5 HEPES, and 0.001% phenol red indicator, pH 7.4) containing 0.5 mg/ml trypsin (type XI; Sigma, St. Louis, MO), tissue chunks were moved to dissociation medium containing no trypsin but 1 mg/ml bovine serum albumin (Sigma) and 1 mg/ml trypsin inhibitor (type II-S; Sigma). Each time cells were needed, two or three chunks were picked and triturated to release single neurons.

### Whole-cell recording

The dissociated neurons were put in a recording chamber containing Tyrode's solution (in mM, 150 NaCl, 4 KCl, 2 $MgCl_2$, 2 $CaCl_2$, and 10 HEPES, pH 7.4). Whole-cell voltage-clamp recordings were obtained using pipettes that were pulled from borosilicate micropipettes (OD 1.55–1.60 mm; Hilgenberg, Malsfeld, Germany), fire polished, and coated with Sylgard (Dow-Corning, Midland, MI). Except for the experiments recording $Na^+$ current (Fig. 2 *B*), the pipettes were filled with the standard internal solution containing (in mM) 75 KCl, 75 KF, 2 $MgCl_2$, 5 HEPES, and 5 EGTA (pH adjusted to 7.4 by KOH). For the experiments recording $Na^+$ current, the same components as in the standard internal solution were used, except that (in mM) 75 KCl + 75 KF was replaced by 75 CsCl + 75 CsF, and the pH was adjusted to 7.4 with CsOH. The seal was formed and the whole-cell configuration was obtained in Tyrode's solution. The cell was then lifted from the bottom of the chamber and moved in front of an array of flow pipes (Microcapillary, content 1 $\mu$l, length 64 mm; Hilgenberg) emitting external recording solutions. The external solutions were basically Tyrode's solution with 30 mM tetraethylammonium (TEA) (to block the delayed rectifier $K^+$ currents) and different concentrations (3 $\mu$M to 3 mM) of $ZnCl_2$. Except for the experiments recording $Na^+$ currents, all external solutions also contained 0.5 $\mu$M tetradotoxin. The $Ca^{2+}$ currents in this preparation tended to run down so quickly and completely (possibly because of the fluoride ions in the internal solution) that hardly any $Ca^{2+}$ currents were detectable ~3 min after establishment of the whole-cell configuration. Some sustained or "late" $K^+$ currents also decreased in a few minutes, presumably because of the reduction of $Ca^{2+}$-dependent $K^+$ currents when the intracellular space was dialyzed with EGTA. We therefore spared organic or inorganic $Ca^{2+}$ channel blockers to avoid unnecessary drug interaction or modulation of the $K_A$ currents. The transient $K^+$ current isolated by these strategies seems to be quite homogeneous. It is 4-aminopyridine sensitive (data not shown) and is blocked by imipramine with features of a simple bimolecular reaction (Kuo, 1998). Furthermore, it shows very similar activation and inactivation kinetics to a group of "fast recovery" $K^+$ current, which recovers quickly from inactivation and thus could be elicited by a positive test pulse after a 50-ms prepulse to −120 mV with a holding potential at −50 mV (Wooltorton and Mathie, 1993; Kuo, 1998). On the other hand, the late (sustained) part of the remaining current seems less homogeneous and probably represents a mixture of residual delayed rectifier and other noninactivating $K^+$ currents as well as

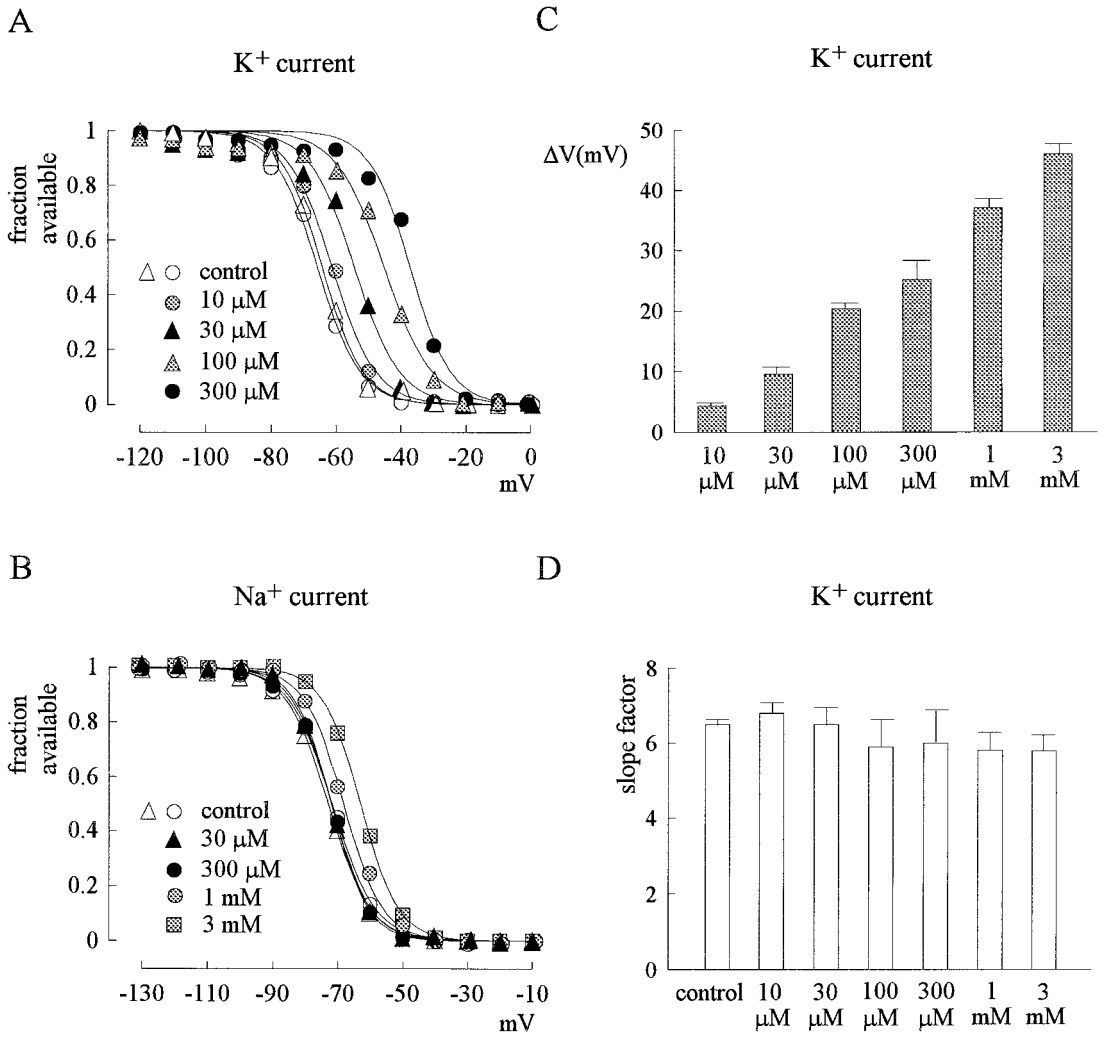


FIGURE 2 Shift of the inactivation curve of $K_A$ and $Na^+$ currents by $Zn^{2+}$. (*A*) Shift of the $K_A$ current inactivation curve by $Zn^{2+}$. The cell was held at −110 mV and stepped every 2 s to the inactivating pulse (−120 to 0 mV) for 200 ms. The $K_A$ current that remains available after each inactivating pulse was assessed by the transient current (the difference between the early peak and the late sustained part of the current) in the following test pulse to +50 mV for 100 ms. The fraction available is defined as the normalized transient current (relative to the transient current after an inactivating pulse at −120 mV) and is plotted against the voltage of the inactivating pulse. Two sets of control data were obtained before and after the four sets of data in 10, 30, 100, and 300 $\mu$M $Zn^{2+}$ to ensure that there was no significant voltage drift during this long experiment. The lines are fits of a Boltzmann function $1/(1 + \exp((V - Vh)/k))$, with *Vh* values (in mV) of −65.7, −66.5, −61.2, −54.3, −45.2, and −37.2 and *k* values of 6.6, 5.9, 6.7, 6.9, 7.4, and 6.2 for control (before $Zn^{2+}$), control (after $Zn^{2+}$), and 10, 30, 100, and 300 $\mu$M $Zn^{2+}$, respectively. (*B*) The inactivation curve of $Na^+$ current. The pulse protocol and the fraction available are the same as in *A*, except that the cell is stepped to a test pulse of 0 mV for 5 ms to assess the $Na^+$ current available. The lines are also fits of a Boltzmann function, with *Vh* values (in mV) of −71.8, −72.0, −72.9, −72.0, −68.2, and −63.0 and *k* values of 6.7, 5.7, 6.5, 6.0, 6.0, and 5.9 for control (before $Zn^{2+}$), control (after $Zn^{2+}$), and 30 $\mu$M, 300 $\mu$M, 1 mM, and 3 mM $Zn^{2+}$, respectively. (*C*) $Zn^{2+}$ concentration-dependent shift of the midpoint ($V_h$) of the $K_A$ current inactivation curve. The shifts ($\Delta V$, in mV) are 4.4 ± 0.23, 9.5 ± 1.2, 20.4 ± 0.92, 25.2 ± 3.0, 37.0 ± 1.4, and 46.0 ± 1.5 ($n$ = 3–4), for 10 $\mu$M, 30 $\mu$M, 100 $\mu$M, 300 $\mu$M, 1 mM, and 3 mM $Zn^{2+}$, respectively. (*D*) The slope factor *k* is not changed by $Zn^{2+}$. Average values of *k* in control, 10 $\mu$M, 30 $\mu$M, 100 $\mu$M, 300 $\mu$M, 1 mM, and 3 mM $Zn^{2+}$ are 6.5 ± 0.15, 6.8 ± 0.29, 6.5 ± 0.45, 5.9 ± 0.75, 6.0 ± 0.90, 5.8 ± 0.50, and 5.8 ± 0.42 ($n$ = 3–4), respectively.

"steady-state" $K_A$ current. We therefore have focused our experimental observation on the transient current to avoid compromise of the experimental results by other heterogeneous currents in the neuron. Currents were recorded at room temperature (~25°C) with an Axoclamp 200A amplifier, filtered at 5 kHz with a four-pole Bessel filter, digitized at 50–200-$\mu$s intervals, and stored using a Digidata-1200 analog/digital interface with pCLAMP software (Axon Instruments, Foster City, CA). Residual series resistance was generally smaller than 1 MΩ after partial compensation (typically >80%). All statistics are given as mean ± standard error of mean.

## RESULTS

### The shift of the $K_A$ current inactivation curve is not saturated in 1–3 mM $Zn^{2+}$

Fig. 1, *A* and *B*, shows that $Zn^{2+}$ inhibits $K_A$ current elicited from negative holding potentials yet enhances $K_A$ current elicited from relatively positive holding potentials. The enhancement effect has been ascribed to the positive shift of

the $K_A$ channel inactivation curve in the voltage axis by $Zn^{2+}$. Harrison et al. (1993) and Davidson and Kehl (1995) presumed saturation of the shift in high $Zn^{2+}$ concentrations and fitted a Hill equation to the shift in different concentrations of $Zn^{2+}$ to obtain a dissociation constant of 14–93 $\mu$M between $Zn^{2+}$ and the $K_A$ channel. However, Bardoni and Belluzzi (1994) did not observe saturation of the shift, even in millimolar $Zn^{2+}$. Because saturation of the shift is an important phenomenon predicted by the modal gating hypothesis (Fig. 1 *C*), we first reexamine in more detail the inactivation curve shift produced by $Zn^{2+}$. Fig. 2 *A* demonstrates that the shift is evident in 10 $\mu$M $Zn^{2+}$ and gets larger with higher concentrations of $Zn^{2+}$. To rule out any "nonspecific" (e.g., surface charge) effect of $Zn^{2+}$, we also examined the effect of $Zn^{2+}$ on the inactivation curve of $Na^+$ channels in the same cells, where there is no shift until the $Zn^{2+}$ concentration reaches millimolar level (Fig. 2 *B*). The effect of $Zn^{2+}$ thus seems to be specific to $K_A$ channels, at least for 300 $\mu$M or lower concentrations of $Zn^{2+}$.

According to the modal gating hypothesis (Fig. 1 *C*), the evident shift of the inactivation curve in 10 $\mu$M $Zn^{2+}$ implies that the binding of 10 $\mu$M $Zn^{2+}$ to the $K_A$ channels is not negligible, or the dissociation constant between $Zn^{2+}$ and the $K_A$ channel is not much larger than 10 $\mu$M. Thus it is likely that in 300 $\mu$M $Zn^{2+}$ most channels are in mode Z (Fig. 1 *C*) and the shift of inactivation curve becomes saturated. This is clearly not the case in Fig. 2 *C*, where the shift is not saturated at concentrations as high as 3 mM $Zn^{2+}$. Even if one ascribes the shift of inactivation curve of $Na^+$ channels in 1 and 3 mM $Zn^{2+}$ (~4 and ~9 mV, respectively; Fig. 2 *B*) to a nonspecific effect and subtracts it from the corresponding data in Fig. 2 *C*, the shift of the $K_A$ channel inactivation curve in 1 and 3 mM $Zn^{2+}$ is still not saturated. Moreover, if channels are distributed in two modes of inactivation in the presence of $Zn^{2+}$, the inactivation curve in $Zn^{2+}$ should be the weighted summation of two different Boltzmann functions. In this regard, it is interesting to note that the inactivation curves in 0–300 $\mu$M $Zn^{2+}$ can all be reasonably fitted by single Boltzmann functions with very similar slope factors (Fig. 2, *A* and *D*). Even if the differently weighted summation of two different Boltzmann functions can always be approximated by a single Boltzmann fit, it is unlikely that the slope factor of the fitted curve always remains the same. The findings in Fig. 2 thus are not well in line with the modal gating hypothesis.

## $Zn^{2+}$ selectively binds to the deactivated state of neuronal $K_A$ channels with a dissociation constant of ~3 $\mu$M

The findings in Fig. 2 suggest that one cannot disregard changes between $Zn^{2+}$-free and $Zn^{2+}$-bound channels while discussing changes between the resting and the inactivated channels. In other words, it seems that $Zn^{2+}$ binding-unbinding does not happen on a much slower time scale than $K_A$ channel gating. Moreover, the prominent shift of the inactivation curve itself suggests a very different affinity between $Zn^{2+}$ and different gating states of $K_A$ channels. We thus depict another simplified gating scheme consisting of the resting and inactivated channels bound by $Zn^{2+}$ or not (states R, I, RZn, IZn; Fig. 3 *A*). Because the steady-state inactivation curve in control can be approximated by a

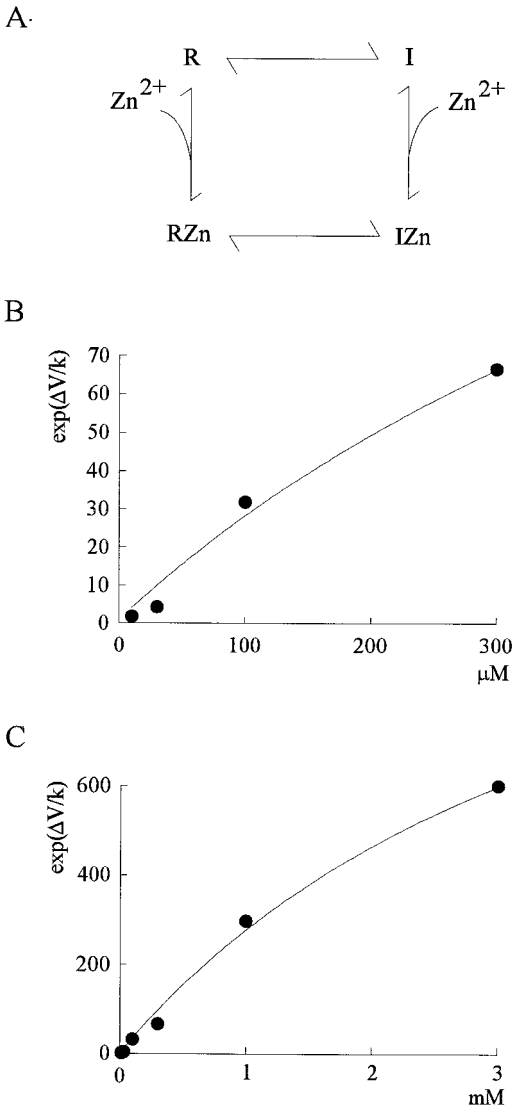


FIGURE 3 Determination of the affinity between $Zn^{2+}$ and neuronal $K_A$ channels by $\Delta V/k$. (*A*) A simplified gating scheme consisting of only the resting (R) and the inactivated (I) channels. $Zn^{2+}$ binds to different gating states with different affinity. (*B*) $\exp(\Delta V/k)$ is plotted against $Zn^{2+}$ concentration. $\Delta V/k$ values are derived from the mean values in Fig. 2, *C* and *D*. The line is a best fit to the data of the form $\exp(\Delta V/k) = (1 + (Zn/3.2\ \mu M))/(1 + (Zn/700\ \mu M))$, where Zn denotes $Zn^{2+}$ concentration. (*C*) A plot similar to that in *B*, with the data of 1 and 3 mM $Zn^{2+}$ included. Again the data in Fig. 2, *C* and *D*, are used, but now 4 and 9 mV (for 1 and 3 mM $Zn^{2+}$, respectively; assessed by the shift of the inactivation curve of $Na^+$ current) are subtracted from the $\Delta V$ values in Fig. 2 *C* to correct for the presumable nonspecific or surface charge effect of millimolar $Zn^{2+}$ on $\Delta V$. The line is a fit to the data of a form similar to that in *B*: $\exp(\Delta V/k) = (1 + (Zn/2.9\ \mu M))/(1 + (Zn/4.1\ mM))$.

Boltzmann distribution, $1/(1 + \exp((V - Vh)/k)$ (see Fig. 2 *A*), the relative steady-state occupancies of state R and state I are described by 1 and $\exp((V - Vh)/k)$, respectively. When $Zn^{2+}$ is added, the relative steady-state occupancies of state RZn and state IZn would be $Zn/K_d(R)$ and $(\exp((V - Vh)/k))*Zn/K_d(I)$, where Zn denotes concentration of $Zn^{2+}$, and $K_d(R)$ and $K_d(I)$ are the dissociation constants of $Zn^{2+}$ to the resting and inactivated states of the channel, respectively.

The steady-state inactivation curve in the presence of $Zn^{2+}$ then would be

$$\% \text{ available channels} = (R + RZn)/(R + I + RZn + IZn)$$

$$= \frac{1 + Zn/K_d(R)}{1 + Zn/K_d(R) + \left[\exp\frac{(V - Vh)}{k}\right] * (1 + Zn/K_d(I))}$$

$$= \frac{1}{1 + \left[\exp\frac{(V - Vh)}{k}\right] * \frac{(1 + Zn/K_d(R))}{(1 + Zn/K_d(I))}}$$

The steady-state inactivation curve in the presence of $Zn^{2+}$ thus will have the same slope as that in control, but shifted to the right by $\Delta V$, with $\exp(\Delta V/k)$ equal to $(1 + (Zn/K_d(R)))/(1 + (Zn/K_d(I)))$. This is consistent with the experimental findings in Fig. 2 *D*, where the inactivation curves all have very similar slope factors. Further quantitative analysis based on the $\exp(\Delta V/k)$ values in 10–300 $\mu$M $Zn^{2+}$ yields a $K_d(R)$ of ~3.2 $\mu$M and a $K_d(I)$ 200 times higher (Fig. 3 *B*). To have a better estimate of the very high $K_d(I)$, $\exp(\Delta V/k)$ values in 1 and 3 mM $Zn^{2+}$ are included after the presumable nonspecific effect of 1 and 3 mM $Zn^{2+}$ on $\Delta V$ is corrected for (4 and 9 mV, respectively, given by the shift of the inactivation curve of $Na^+$ current in Fig. 2 *B*). The results are plotted in Fig. 3 *C*, which shows a $K_d(R)$ of ~2.9 $\mu$M and a $K_d(I)$ of ~4.1 mM. This $K_d(R)$ value is quite consistent with that in Fig. 3 *B* (3.2 $\mu$M). Although 4.1 mM may still be a rough estimate of $K_d(I)$, it is evident that $Zn^{2+}$ selectively binds to the resting state of the central neuronal $K_A$ channel, and $K_d(I)$ is much (a few hundred to 1000-fold) higher than $K_d(R)$.

## At +40 mV most $Zn^{2+}$ has unbound from the $K_A$ channel before the channel is open

Other than shift of the inactivation curve, the other major effect of $Zn^{2+}$ on $K_A$ channel gating is slowing of activation (Harrison et al., 1993; Bardoni and Belluzzi, 1994). We have argued that the kinetics of $Zn^{2+}$ action probably is not slow enough to justify the use of the modal-gating hypothesis. Because activation seems to have faster kinetics than inactivation (the time constant of monoexponential fit to the rising phase of current to the peak is ~0.48 ms at +40 mV, whereas the time constant of the decay phase of current is ~11.5 ms; see Fig. 5), it would be interesting to see whether this hypothesis is also inappropriate for explaining the effect of $Zn^{2+}$ on channel activation. Here we choose to measure the initial delay of activation to represent the effect of $Zn^{2+}$ on $K_A$ channel activation because in later phases the activation process tends to be more mingled with the inactivation process. Fig. 4, *A* and *B*, demonstrates that at +40 mV the initial delay is already lengthened in 10 $\mu$M $Zn^{2+}$, yet is still getting longer in 1 mM $Zn^{2+}$, showing no signs of saturation. This finding is incompatible with the modal gating hypothesis, which would predict a saturated initial delay at high concentrations of $Zn^{2+}$.

To explain the effect of $Zn^{2+}$ on $K_A$ channel activation, a more elaborated gating scheme is plotted in Fig. 4 *C*. If the dissociation constant between $Zn^{2+}$ and the resting (fully deactivated) channels is ~3 $\mu$M, then in 10 $\mu$M or higher $Zn^{2+}$ most $K_A$ channels would be in state CZn at the end of the hyperpolarizing interpulse interval. Upon membrane depolarization the channels in state CZn could be activated via two different routes, the CZn-C-O route or the CZn-OZn-O route. Here we have a route of CZn-OZn-O rather than CZn-OZn, because OZn would mostly (and probably also quickly) turn into O in view of the low affinity between open $K_A$ channels and $Zn^{2+}$. Moreover, if the $Zn^{2+}$ binding site is in the pore (see Discussion), $Zn^{2+}$ binding may block $K^+$ permeation and thus state OZn may be nonconducting. If CZn-OZn-O is the major route of activation, the activation kinetics are most likely determined by the CZn-to-OZn rate, and thus the initial delay of channel activation would not be very different in 10 $\mu$M to 1 mM $Zn^{2+}$. On the other hand, if CZn-C-O is the major route, and if the C-to-CZn transition ($Zn^{2+}$ binding) effectively competes with the C-to-O transition for channels in state C (i.e., the C-to-CZn rate is not much slower than the C-to-O rate), then there may be different slowing of $K_A$ channel activation in different concentrations of $Zn^{2+}$. The effect of the C-to-CZn transition will be more evident when the CZn-to-C rate is slower (than the C-to-O rate). This is as if the CZn-to-C transition were the rate-limiting step of the serial activation "reaction," and the C-to-CZn transition slows the activation by driving channels in state C back to state CZn to repeat the rate-limiting step. The concentration-dependent initial delay in Fig. 4 therefore strongly suggests that the CZn-C-O route is the major pathway of activation at +40 mV. In other words, most $Zn^{2+}$ seems to have unbound before the $K_A$ channel is open at +40 mV. The "competition" between the C-to-O transition and the C-to-CZn transition also implies that the C-to-CZn rate is not much slower than the C-to-O rate, arguing against the basic assumption of the modal gating hypothesis (see Fig. 1 *C*).

## Similar peak current inhibition by 0.1–1 mM $Zn^{2+}$ at very positive potentials

The transition between states CZn and OZn (and that between states C and O) involves intrinsic gating processes of the channel and thus is probably strongly voltage dependent. On the other hand, the binding and unbinding of

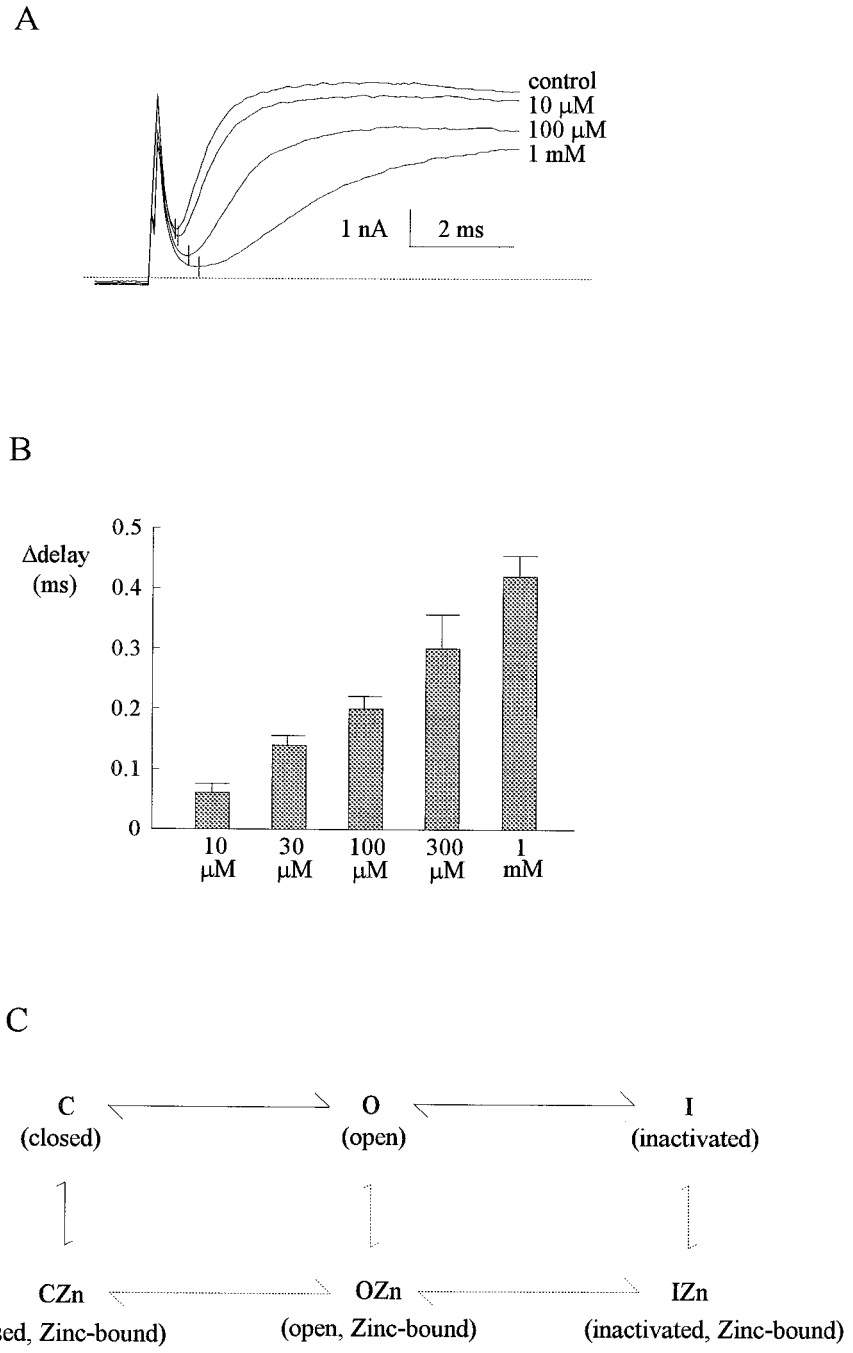


FIGURE 4 Slowing of $K_A$ channel activation by $Zn^{2+}$. (*A*) The cell was stepped to +40 mV from a holding potential of −110 mV to elicit the $K_A$ current. The dashed line denotes zero current level. Note the dose-dependent slowing of the activation phase with lengthening of the initial delay (marked by short vertical lines in the sweeps) by 10 $\mu$M, 100 $\mu$M, and 1 mM $Zn^{2+}$. The initial delay is defined as the first sampling point where the next three consecutive points all show increasing current, and the current is considered as increasing when the increment of current between two consecutive sampling points exceeds 10% of the largest increment between two consecutive points in that sweep. (*B*) At +40 mV, the differences between the initial delay in the control condition and the initial delay in the presence of $Zn^{2+}$ are (Δdelay, in ms) 0.06 ± 0.015, 0.14 ± 0.018, 0.20 ± 0.019, 0.30 ± 0.058, and 0.42 ± 0.035 ($n$ = 4–7) in 10 $\mu$M, 30 $\mu$M, 100 $\mu$M, 300 $\mu$M, and 1 mM $Zn^{2+}$, respectively. (*C*) A new gating scheme consisting of closed (C), open (O), and inactivated (I) states of the $K_A$ channels. Binding and unbinding of $Zn^{2+}$ to and from each of these states are again individually considered. The solid and dashed arrows denote, respectively, the favored and unfavored routes of activation at +40 mV (see text for details).

external $Zn^{2+}$ to and from the deactivated channel presumably have little or no voltage dependence because the pore is closed and nonconducting. If these assumptions are true, then at very positive potentials the CZn-to-OZn rate may be significantly faster than the CZn-to-C rate, and CZn-OZn-O becomes the major route of activation. According to the foregoing argument on the concentration-dependent initial delay, the delay would then become less sensitive to $Zn^{2+}$ concentration at very positive potentials. Fig. 5 *A* shows the activation phase of $K_A$ current in different concentrations of $Zn^{2+}$ at +40 and +120 mV. The initial delay at +120 mV is much shorter than that in +40 mV and is clearly much less different in different $Zn^{2+}$ concentrations. Moreover, it is interesting to note that the inhibition of peak $K_A$ current is different in different concentrations of $Zn^{2+}$ at +40 mV, yet becomes more similar in different concentrations of $Zn^{2+}$ at +120 mV. Because the decreased peak $K_A$ current by $Zn^{2+}$ is ascribable to the slowed activation with an unchanged inactivation rate (the macroscopic inactivation rate of $K_A$ current is not changed by $Zn^{2+}$; Bardoni and Belluzzi, 1994; see also Fig. 5 *B*), similar peak current inhibition by 100 $\mu$M to 1 mM $Zn^{2+}$ at +120 mV would also suggest that $Zn^{2+}$ binding no longer has a significant effect on the kinetics of $K_A$ channel activation at +120 mV.

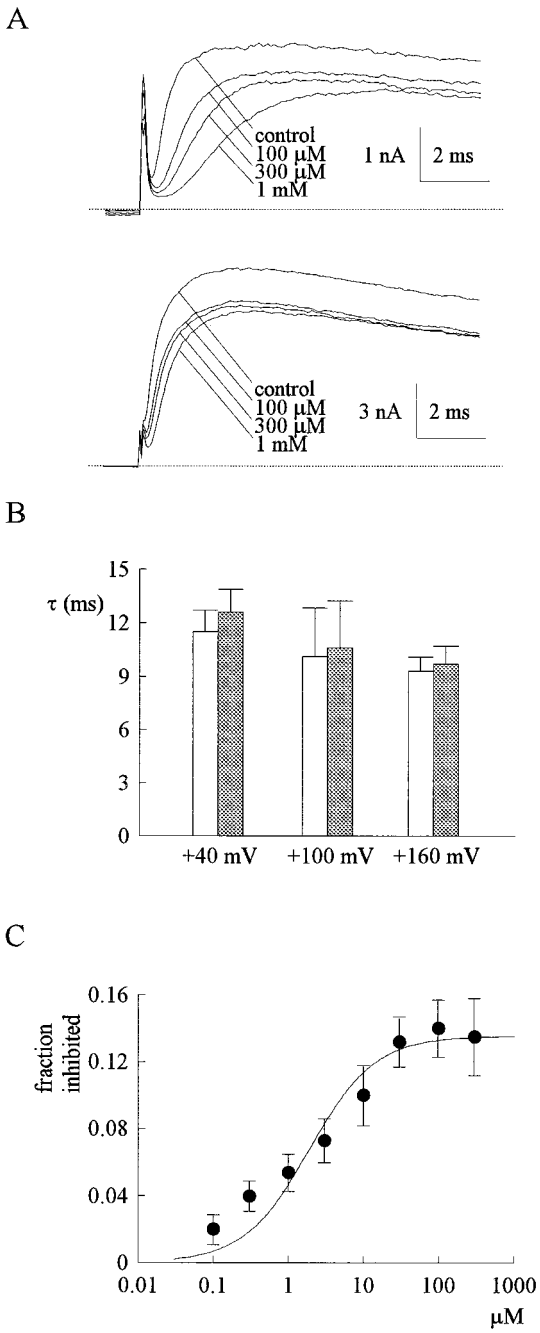


FIGURE 5 Effect of $Zn^{2+}$ on $K_A$ channel at very positive potentials. (*A*) The cell was stepped to +40 mV (*upper panel*) or +120 mV (*lower panel*) from a holding potential of −110 mV to elicit the $K_A$ current in control, 100 μM, 300 μM, and 1 mM $Zn^{2+}$. The dashed lines denote zero current level. Note that the initial delay is much shortened at +120 mV. Although the initial delay and the inhibition of peak $K_A$ current are still slightly more prominent in 1 mM than in 100 μM $Zn^{2+}$, the differences are much smaller than that at +40 mV. (*B*) The cells were stepped to +40 ~ +160 mV from a holding potential of −110 mV to elicit the $K_A$ current, and the decaying phase of macroscopic $K_A$ current is fitted by monoexponential functions. The decaying time constants are similar whether $Zn^{2+}$ is present or not. In the control conditions (*white bars*) the time constants are 11.5 ± 1.2 (+40 mV), 10.1 ± 2.7, and 9.3 ± 0.8 ms at +40, +100, and +160 mV, respectively. In the presence of 100 μM $Zn^{2+}$ (*gray bars*), the time constants are 12.6 ± 1.3 (+40 mV), 10.6 ± 2.7, and 9.7 ± 1.0 ms at +40, +100, and +160 mV, respectively. (*C*) The cell was stepped to +140 mV from a holding potential of −110 mV to elicit the $K_A$ current. The difference between the peak currents in control and in the presence of $Zn^{2+}$ is divided by the peak current in control to give the "fraction inhibited," which is then plotted against $Zn^{2+}$ concentration. The line is a best fit to the data points of the form: fraction inhibited = 0.14[(Zn/1.9 μM)/(1 + (Zn/1.9 μM))], where Zn denotes $Zn^{2+}$ concentration.

This is probably due to the fact that at very positive potentials the CZn-to-C transition is effectively antagonized by the CZn-to-OZn transition and CZn-OZn-O becomes the major pathway. Even if some channels in state CZn still take the CZn-to-C route of activation at +120 mV, they will be "absorbed" by the very fast C-to-O transition as soon as they reach the C state (i.e., the C-to-CZn transition becomes negligible as it is effectively antagonized by the C-to-O transition). The slowing of activation and, consequently, the peak current inhibition thus are far less dependent on $Zn^{2+}$ concentration at +120 mV than at +40 mV.

If at very positive potentials the CZn-to-OZn and C-to-O transitions become so fast that the C-to-CZn ($Zn^{2+}$ binding) step no longer contributes significantly to the slowing of activation, the slowing of activation and, consequently, the peak current inhibition by $Zn^{2+}$ should be correlated with the proportion of channels in state CZn and state C at the end of the hyperpolarizing interpulse interval. Fig. 5 *C* plots the peak current inhibition versus $Zn^{2+}$ concentration at very positive potentials (+140 mV). The data can be reasonably described by a one-to-one binding curve with a dissociation constant ($K_d$) of 1.9 μM. This is very close to the $K_d$ obtained with a totally different approach in Fig. 3. All together, these findings argue that the inhibition of $K_A$ current by $Zn^{2+}$ could be explained by purely kinetic considerations, and that $Zn^{2+}$ selectively binds to the closed $K_A$ channel with a $K_d$ of ~3 μM.

## The effect of $Zn^{2+}$ on the $K_A$ current is mimicked by $Cd^{2+}$ but not by $Ni^{2+}$

In Fig. 4 we have argued that the $Zn^{2+}$ binding (C-to-CZn transition) probably is fast enough to compete with channel activation (C-to-O transition) at +40 mV. The relatively fast $Zn^{2+}$ binding rate implies a large capture radius of the $Zn^{2+}$ binding site (Berg, 1983; Hille, 1992). The $Zn^{2+}$ binding site in the $K_A$ channel therefore may not be a rigid cavity that just fits the incoming $Zn^{2+}$ ion. $Cd^{2+}$ is larger than $Zn^{2+}$ but has a similar electronic shell. $Ni^{2+}$, on the other hand, is similar to $Zn^{2+}$ in size but dissimilar in the electronic shell. Fig. 6 *A* shows that $Cd^{2+}$ has an action similar to that of $Zn^{2+}$ in enhancing the $K_A$ current elicited from a holding potential of −70 mV, whereas $Ni^{+2}$ has little effect. Fig. 6, *B* and *C*, shows that 300 μM $Cd^{2+}$ and 300 μM $Zn^{2+}$ both markedly shift the inactivation curve of $K_A$ current, but the shift in 300 μM $Ni^{2+}$ is much smaller. The similar action of $Cd^{2+}$ (but not $Ni^{2+}$) to $Zn^{2+}$ suggests that the electron configuration of the ion is much more important than ion size in determining the effectiveness of binding and

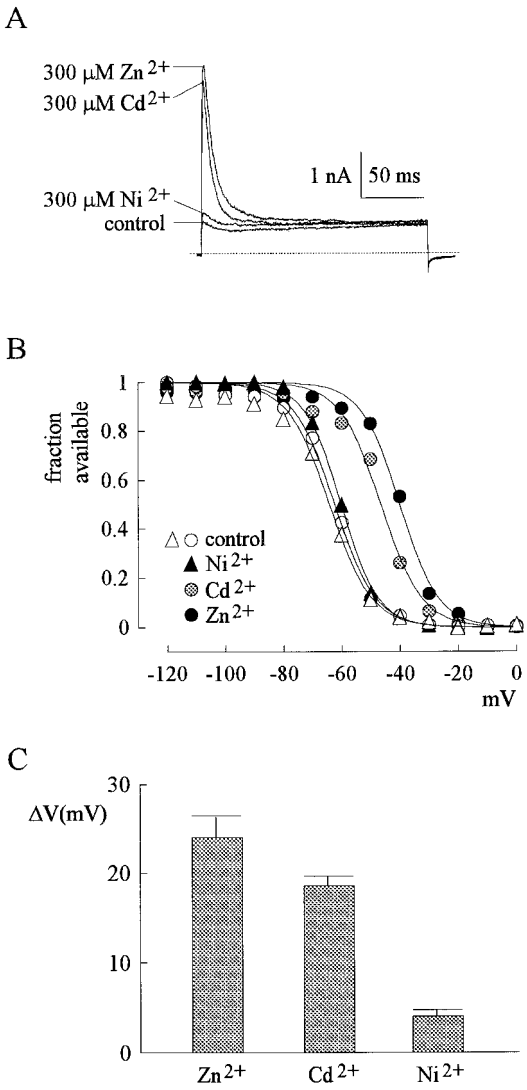


FIGURE 6 The effect of 300 $\mu$M $Zn^{2+}$, $Cd^{2+}$, or $Ni^{2+}$ on $K_A$ current. (*A*) The cell was held at $-70$ mV and stepped to $+50$ mV for 180 ms. Note the significant enhancement of the $K_A$ current by $Zn^{2+}$ and $Cd^{2+}$, but not by $Ni^{2+}$. The dashed line denotes zero current level. (*B*) Shift of the $K_A$ current inactivation curve by $Zn^{2+}$, $Cd^{2+}$, and $Ni^{2+}$. Experiments similar to those in Fig. 2 *A* to demonstrate a shift of the inactivation curve ($\Delta V$) by 300 $\mu$M $Zn^{2+}$, $Cd^{2+}$, and $Ni^{2+}$. The lines are fits of a Boltzmann function $1/(1 + \exp((V - Vh)/k))$, with *Vh* values (in mV) of $-63.6$, $-62.4$, $-40.0$, $-46.6$, and $-60.2$ and *k* values of 7.0, 6.8, 6.6, and 6.3 for two controls, 300 $\mu$M $Zn^{2+}$, $Cd^{2+}$, and $Ni^{2+}$, respectively. (*C*) Shift of the midpoint ($V_h$) of the $K_A$ current inactivation curve by different ions. The shifts ($\Delta V$, in mV) are 24.04 $\pm$ 2.44, 18.64 $\pm$ 1.02, and 3.99 $\pm$ 0.83 for 300 $\mu$M $Zn^{2+}$, $Cd^{2+}$, and $Ni^{2+}$, respectively.

therefore supports the view that the $Zn^{2+}$ binding site is not a fixed rigid cavity (see Discussion).

## DISCUSSION

### The binding and unbinding rates of $Zn^{2+}$

We have demonstrated that $Zn^{2+}$ selectively binds to the deactivated $K_A$ channels with a dissociation constant of $\sim$3 $\mu$M. Although it is difficult to have a direct measurement of the kinetics of $Zn^{2+}$ action on deactivated channels, we could still have an estimate based on an analysis of the interactions between $Zn^{2+}$ and channel gating. Here we choose to present an analytical approach at $+120$ mV (Fig. 7B), because at more positive potentials it would be more justified to neglect the very small leftward arrows (intrinsic deactivation rates) and simplify the analysis. Experimentally in the control condition the activation time constant of $K_A$ channels at $+120$ mV is $\sim$0.32 ms (monoexponential fit to the rising phase of current in Fig. 5 *A*). This could be simulated by an "overall" C1-to-O rate (Fig. 7 *B*, or the C-to-O rate in Fig. 4 *C*) of 2500 $s^{-1}$ and an O-to-I rate of 100 $s^{-1}$ (calculation using the four-order Runge-Kutta method). An overall C1-to-O rate of 2500 $s^{-1}$ would mean that every step leading from C1 to O cannot be slower than 2500 $s^{-1}$ (actually if one step is 2500 $s^{-1}$, then all of the other steps must be quite faster than 2500 $s^{-1}$). To produce a "saturating" peak current inhibition of $\sim$15% with slowed activation and an unchanged inactivation rate in the presence of $Zn^{2+}$ (Fig. 5, *B* and *C*), computer simulation indicates that the slowest step in the route leading from C1Zn to O should be at least 800 $s^{-1}$. With the lowest estimates (a C2-to-O rate of 2500 $s^{-1}$ and a C2Zn-to-C2 rate of 800 $s^{-1}$) in the presumed major activation route C1Zn-C2Zn-C2-O at $+120$ mV (see also the legend of Fig. 7), computer simulations show that the peak current inhibition and the initial delay remain almost the same for different C2-to-C2Zn rates up to 300 $s^{-1}$. If the C2-to-C2Zn rate is increased to 1000 $s^{-1}$, the peak current is only slightly more inhibited and the delay slightly more lengthened. This is very similar to the 300 $\mu$M to 1 mM $Zn^{2+}$ data in Fig. 5 *A* and thus indicates a $Zn^{2+}$ binding rate to C2 of $\sim 10^6$ $M^{-1}$ $s^{-1}$. This should be viewed as a low estimate. For example, if the C2-to-O and C2Zn-to-C2 rates are increased 10 times, then the C2-to-C2Zn rate ($Zn^{2+}$ binding rate to C2) can also be increased 10 times to keep the results almost the same. Furthermore, the rate of binding to C1 probably should be even faster than the rate of binding to C2. The binding rate of $Zn^{2+}$ to the deactivated $K_A$ channels thus seems to be quite fast.

### The nature of the $Zn^{2+}$ binding site in neuronal $K_A$ channels

Metal-binding sites in metalloproteins can be categorized as either catalytic or structural. The catalytic role of $Zn^{2+}$ is exemplified in metalloenzymes such as carbonic anhydrase, carboxypeptidase, and alkaline phosphatase. In such cases the highly localized charge and electron affinity (strong Lewis acid) of $Zn^{2+}$ contribute to a very effective attacking group, and $Zn^{2+}$ is tightly bound to the active site (usually with a dissociation constant in the nanomolar range). The site is often located in $\beta$ sheet structures, the rigidity of which contributes to the tight binding and prevents exchange of metal ions. The other type of metal-binding site, the structural type, tends to impose a specific conformation

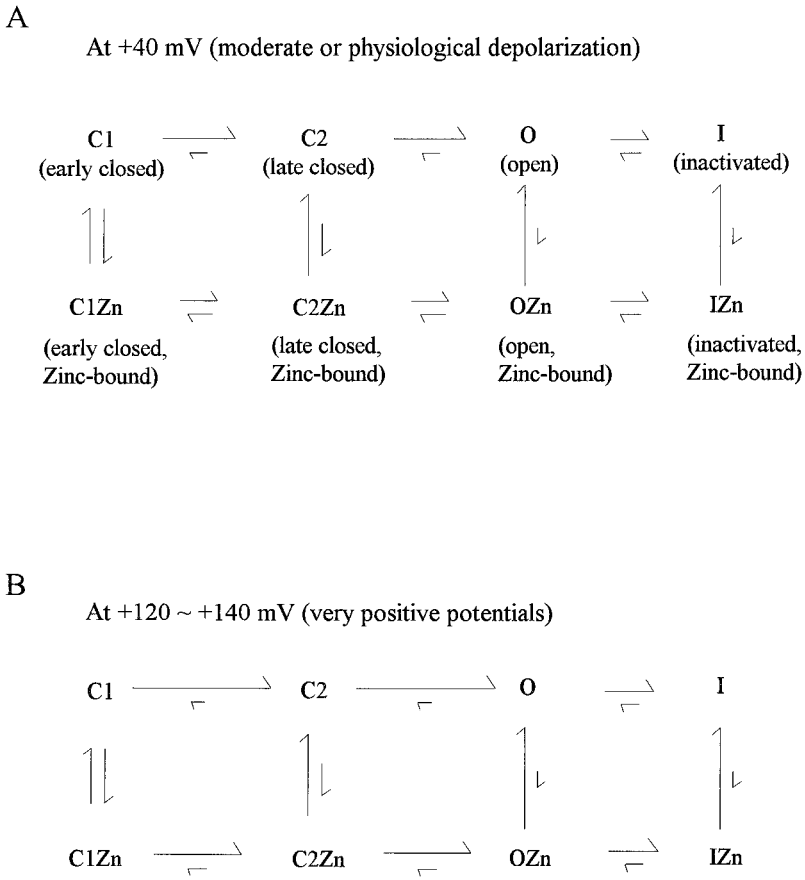


FIGURE 7 Semiquantitative schemes summarizing $Zn^{2+}$ action on neuronal $K_A$ channels. (*A*) A gating scheme at +40 mV (moderate or physiological depolarizations) is modified from that in Fig. 4 *C* with one more closed states added. To keep the scheme simple and intuitive, we make no attempt to fit the initial delay by adding more closed states. The length of the arrows roughly represents the relative speed of each transition. A certain constant $Zn^{2+}$ concentration is assumed throughout the figure, and thus the dependence of the $Zn^{2+}$ binding rate on $Zn^{2+}$ concentration is not illustrated. $Zn^{2+}$ binding is fastest to C1 (early closed state) and is slower to state C2 (late closed state) and even slower to state O, whereas there is an opposite trend for the unbinding rate of $Zn^{2+}$. These differences reflect the different affinity between the resting and the inactivated state (states I and O are assumed to have the same affinity for $Zn^{2+}$ to emphasize the affinity change during the activation process). The C1Zn-to-C1 rate is faster than the C1Zn-to-C2Zn rate, and the C1-to-C1Zn rate is not much slower than the C1-to-C2 rates. On the other hand, the C1Zn-to-C1 transition is somewhat slower than the C1-to-C2 transition and thus is at least a partial rate-limiting step of the overall activation processes in the presence of $Zn^{2+}$. These kinetic parameters make C1Zn-C1-C2-O a major route of activation at +40 mV and significant correlation between the slowing of activation (or inhibition of peak current) and $Zn^{2+}$ concentration. (*B*) A gating scheme similar to that in *A*, but at very positive potentials (+120 to +140 mV). The vertical arrows are unchanged, whereas the rightward arrows are greatly lengthened and the reverse (leftward) arrows are shortened (except for the arrows between states O and I and between OZn and IZn). Because the speeded rightward horizontal transition would more effectively antagonize the vertical arrows, the $Zn^{2+}$ concentration-dependent slowing of channel activation becomes less prominent, and the major activation route is shifted right. For example, C1Zn-C2Zn-C2-O (or even C1Zn-C2Zn-OZn-O) may become the major route of activation now. This point is explained in more detail in an analytical approach in the Discussion, which yields a $K_d$ of ~800 $\mu$M (800 $s^{-1}/10^6$ $M^{-1}$ $s^{-1}$) between $Zn^{2+}$ and C2. This is much higher than the ~3 $\mu$M $K_d$ between $Zn^{2+}$ and the fully deactivated $K_A$ channel (state C1) and is consistent with the idea that the route of activation is shifted right at very positive potentials.

of the protein or enzyme when bound with a metal ion. The structural role of $Zn^{2+}$ is exemplified by zinc finger peptides and insulin. Many of these binding sites have $\alpha$-helical structures, the nonrigid or flexible nature of which makes the binding affinity of $Zn^{2+}$ lower (because of the loss of configurational entropy of the peptide upon binding of the metal ion) and rapid exchange of the metal ion possible (for a review see Williams, 1989; Nieboer and Fletcher, 1996; Berg and Godwin, 1997). The rapid kinetics of $Zn^{2+}$ action along with a dissociation constant of ~ 3 $\mu$M thus are consistent with a binding site of the structural type in the resting (deactivated) neuronal $K_A$ channels. The findings that $Cd^{2+}$ (Pauling radius 0.99 Å) but not $Ni^{2+}$ (0.72 Å) has an effect similar to that of $Zn^{2+}$ (0.74 Å) are also consistent with a flexible nature of the binding site.

## Possible binding ligands in the $Zn^{2+}$-binding site in neuronal $K_A$ channels

Spires and Begenisich (1992) found that histidyl and sulfhydryl group modifying reagents did not change the effect of $Zn^{2+}$ on squid $K^+$ channels. Boland et al. (1994) showed that mutation of all cysteine residues in Shaker $K^+$ channels

did not alter the effect of $Zn^{2+}$. On the other hand, Spires and Begenisich (1994) found that trinitrobenzene sulfonic acid (TNBS) reduced the effect of $Zn^{2+}$ on Shaker $K^+$ channels. TNBS selectively modifies the $\epsilon$-amino group of lysine, which has a pKa value near 9 and is mostly positively charged at neutral pH. This group thus is unlikely to coordinate $Zn^{2+}$ directly but is probably located near the binding site (to prevent $Zn^{2+}$ binding after trinitrobenzene substitution). Other than cysteine and histidine, the most common coordinating ligands for $Zn^{2+}$ in proteins are aspartate or glutamate (for a review see Vallee and Auld, 1990). Although $Ni^{2+}$ and $Zn^{2+}$ are similar in size, they are dissimilar in their electron configuration and coordination chemistry. Both $Ni^{2+}$ and $Zn^{2+}$ may be coordinated by the S atom in thiolate groups and the N atom in imidazole groups. However, only $Zn^{2+}$ is well coordinated by the oxygen atom in carboxylate or carbonyl groups (for a review see Cowan, 1997). The different effects on neuronal $K_A$ channels between $Ni^{2+}$ and $Zn^{2+}$ thus also imply the involvement of oxygen-containing ligands in ion binding. Because effective charge neutralization and liberation of water molecules (increase in entropy) would compensate for the loss of configuration entropy upon ion binding, carboxylate groups are widely used in flexible cation-binding sites with relatively strong affinity as well as rapid on-off rates of the ion (e.g., the high-affinity $Ca^{2+}$-binding site in $Ca^{2+}$ channels; Kuo and Hess, 1993; Yang et al., 1993), which may also fit the above-described nature of the $Zn^{2+}$-binding site in neuronal $K_A$ channels.

## The location of the $Zn^{2+}$-binding site in neuronal $K_A$ channels

In an ion channel, many metal-protein interactions take place in the conduction pathway. Because the $Zn^{2+}$-binding site is conformationally different in the resting and in the open $K_A$ channel, it is tempting to locate the binding site in the pore, which also undergoes conformational changes during channel gating and is well equipped with oxygen-containing ligands (carboxylate and carbonyl groups) suitable for coordinating $Zn^{2+}$. However, it has been shown that 500 $\mu$M $Zn^{2+}$ produced at most a slight reduction in single $K_A$ channel current and little change in the mean open time of the channel (Spires and Begenisich, 1994), which is apparently inconsistent with a $Zn^{2+}$-binding site in the conduction pathway. Yet with the findings in this study that $Zn^{2+}$ has a high affinity for only the deactivated $K_A$ channels, and that the unbinding rate of $Zn^{2+}$ from the open channel may be very fast (in view of the low affinity between $Zn^{2+}$ and the open channels; Fig. 7), those single-channel data should still be compatible with a $Zn^{2+}$-binding site in the pore. Thus there is no conclusive evidence to locate the binding site in or out of the pore at present. If the binding site is outside the pore, it would indicate significant gating conformational changes elsewhere in the channel than in the conduction pathway. If the binding site is in the pore, it most likely is superficially located in view of the fast binding rate of $Zn^{2+}$. In this regard it is interesting to note that the conformation of the external pore mouth of $K_A$ channels seems to change significantly during gating processes such as activation (Kuo, 1998) or C-type inactivation (Hoshi et al., 1991; Choi et al., 1991; Lopez-Barneo et al., 1993; Ogielska et al., 1995; Liu et al., 1996).

## Physiological implications

The concentration of $Zn^{2+}$ in the cerebrospinal fluid is 0.2–0.4 $\mu$M (Gooddy et al., 1974, 1975; Palm and Hallmans, 1982). However, vivid zinc staining is present in many brain areas, including neocortex and hippocampus (Faber et al., 1989; Frederickson, 1989; Perez-Clausell, 1996). Ultrastructural studies have indicated that $Zn^{2+}$ is located within the synaptic vesicles in excitatory boutons (Haug, 1967; Perez-Clausell and Danscher, 1986; Beaulieu et al., 1992), and it has been demonstrated that in the hippocampus $Zn^{2+}$ is released from nerve endings during neural activities (Assaf and Chung, 1984; Aniksztejn et al., 1987). After intense neural activity the extracellular concentration of chelatable $Zn^{2+}$ may be as high as 300 $\mu$M (Assaf and Chung, 1984). The presence of $Zn^{2+}$ uptake mechanisms with binding constants of 12 to 400 $\mu$M in the hippocampus (Howell et al., 1984) also suggests that a few tens micromolar or even higher local extracellular $Zn^{2+}$ concentrations could exist in vivo.

$K_A$ current is important in modulating cellular excitability and the discharge pattern of the cell (for a review see Hille, 1992). The dual effects of $Zn^{2+}$ on neuronal $K_A$ current thus may have dual effects on neuronal activity. When the membrane potential is hyperpolarized, $Zn^{2+}$ inhibits $K_A$ current and thus increases the excitability and firing frequency of the neuron. On the other hand, $Zn^{2+}$ would enhance $K_A$ current and decrease neuronal excitability when the neuronal membrane becomes more depolarized. Because the extracellular $Zn^{2+}$ concentration may change with nerve impulses, $Zn^{2+}$ could be an endogenous negative feedback controller of neural activities. When a neural circuit is hyperactive, the elevated $Zn^{2+}$ concentration along with the relatively depolarized neuronal membrane potential would enhance $K_A$ current and decrease neuronal excitability. In this regard it is interesting to note that $Zn^{2+}$ exerts its effect on $K_A$ currents by rapid and selective binding to the deactivated channels, and that the slowing of activation and shift of the inactivation curve are closely correlated with $Zn^{2+}$ concentration without saturation in up to millimolar $Zn^{2+}$ at moderate (physiological) depolarizations. Different concentrations of $Zn^{2+}$ thus would always have different effects on $K_A$ current and neuronal activities, even if the $Zn^{2+}$ concentration is already much higher than $\sim$3 $\mu$M, the dissociation constant between $Zn^{2+}$ and the deactivated $K_A$ channels. Through its effect on $K_A$ current, $Zn^{2+}$ may act as a faithful "fine tuner" that controls and is controlled by neural activities.

This work was supported by a grant from the National Science Council, Taiwan, R.O.C. (NSC 88-2314-B-002-212).

## REFERENCES


Aniksztejn, L., G. Charton, and Y. Ben-Ari. 1987. Selective release of endogenous zinc from the hippocampal mossy fibers in situ. *Brain Res.* 404:58–64.

Assaf, S. Y., and S.-H. Chung. 1984. Release of endogenous $Zn^{2+}$ from brain tissue during activity. *Nature.* 308:734–736.

Bardoni, R., and O. Belluzzi. 1994. Modifications of A-current kinetics in mammalian central neurons induced by extracellular zinc. *J. Physiol. (Lond.).* 479:389–401.

Beaulieu, C., R. Dyck, and M. Cynadar. 1992. Enrichment of glutamate in zinc-containing terminals of the cat visual cortex. *Neuroreport.* 3:861–864.

Berg, H. C. 1983. Random Walks in Biology. Princeton University Press, Princeton, NJ.

Berg, J. M., and H. A. Godwin. 1997. Lessons from zinc-binding peptides. *Annu. Rev. Biophys. Biomol. Struct.* 26:357–371.

Boland, L. M., M. E. Jurman, and G. Yellen. 1994. Cysteines in the Shaker $K^+$ channel are not essential for channel activity or zinc modulation. *Biophys. J.* 66:694–699.

Choi, K. L., R. W. Aldrich, and G. Yellen. 1991. Tetraethylammonium blockade distinguishes two inactivation mechanisms in voltage-activated $K^+$ channels. *Proc. Natl. Acad. Sci. USA.* 88:5092–5095.

Cowan, J. A. 1997. Fundamentals of inorganic biochemistry. *In* Inorganic Biochemistry: An Introduction. J. A. Cowen, editor. Wiley-VCH, New York. 1–63.

Davidson, J.-L., and S. J. Kehl. 1995. Changes of activation and inactivation gating of the transient potassium current of rat pituitary melanotrophs caused by micromolar $Cd^{2+}$ and $Zn^{2+}$. *Can. J. Physiol. Pharmacol.* 73:36–42.

Faber, H., K. Braun, W. Zuschratter, and H. Scheich. 1989. System specific distribution of zinc in the chick brain: a light and electron-microscopic study using the Timm method. *Cell Tissue Res.* 258:247–257.

Frederickson, C. J. 1989. Neurobiology of zinc and zinc-containing neurons. *Int. Rev. Neurobiol.* 131:145–238.

Frederickson, C. J., M. A. Klitenick, W. I. Manton, and J. B. Kirkpatrick. 1983. Cytoarchitectonic distribution of zinc in the hippocampus of man and the rat. *Brain Res.* 273:335–339.

Gooddy, W., E. I. Hamilton, and T. R. Williams. 1975. Spark-source mass spectrometry in the investigation of neurological disease. II. Element levels in brain, cerebrospinal fluid and blood: some observations on their abundance and significance. *Brain.* 98:65–70.

Gooddy, W., T. R. Williams, and D. Nicholas. 1974. Spark-source mass spectrometry in the investigation of neurological disease. I. Multi-element analysis in blood and cerebrospinal fluid. *Brain.* 97:327–336.

Harrison, N. L., H. K. Radke, G. Talukder, and J. M. H. Ffrench-Mullen. 1993. Zinc modulates transient outward current gating in hippocampal neurons. *Receptors Channels.* 1:153–163.

Haug, F. M. S. 1967. Electron microscopical localization of the zinc in hippocampal mossy fibre synapses by a modified sulphide silver procedure. *Histochemie.* 8:355–368.

Hess, P., and R. W. Tsien. 1984. Mechanism of ion permeation through calcium channels. *Nature.* 309:453–456.

Hille, B. 1992. Potassium channels and chloride channels. *In* Ionic Channels of Excitable Membranes. B. Hille, editor. Sinauer Associates, Sunderland, MA. 116–121.

Hoshi, T., W. N. Zagotta, and R. W. Aldrich. 1991. Two types of inactivation in Shaker potassium channels: effects of alterations in the carboxy-terminal region. *Neuron.* 7:547–556.

Howell, G. A., M. G. Welch, and C. J. Frederickson. 1984. Stimulation-induced uptake and release of zinc in hippocampal slices. *Nature.* 308:736–738.

Huang, R.-C., Y.-W. Peng, and K.-W. Yau. 1993. Zinc modulation of a transient potassium current and histochemical localization of metal in neurons of the suprachiasmatic nucleus. *Proc. Natl. Acad. Sci. USA.* 90:11806–11810.

Kuo, C.-C. 1998. Imipramine inhibition of transient $K^+$ current: an external open-channel blocker preventing fast inactivation. *Biophys. J.* 12: 2845–2857.

Kuo, C.-C., and P. Hess. 1993. Characterization of the high affinity $Ca^{2+}$ binding sites in the L-type $Ca^{2+}$ channel pore in rat phaeochromocytoma cells. *J. Physiol. (Lond.).* 466:657–682.

Liu, Y., M. E. Jurman, G. Yellen. 1996. Dynamic rearrangement of the outer mouth of a $K^+$ channel during gating. *Neuron.* 16:859–867.

Lopez-Barneo, H., T. Hoshi, S. H. Heinemann, and R. W. Aldrich. 1993. Effects of external cations and mutations in the pore region on C-type inactivation of Shaker potassium channels. *Receptors Channels.* 1:61–71.

Nieboer, E., and G. G. Fletcher. 1996. Determinants of reactivity in metal toxicology. *In* Toxicology of Metals. L. W. Chang, editor. CRC Press, Boca Raton, FL. 113–132.

Ogielska, E. M., W. N. Zagotta, T. Hoshi, S. H. Heinemann, J. Haab, and R. W. Aldrich. 1995. Cooperative subunit interactions in C-type inactivation of K channels. *Biophys. J.* 69:2449–2457.

Palm, R., and G. Hallmans. 1982. Zinc concentrations in the cerebrospinal fluid of normal adults and patients with neurological diseases. *J. Neurol. Neurosurg. Psychiatry.* 45:685–690.

Perez-Clausell, J. 1996. Distribution of terminal fields stained for zinc in the neocortex of the rat. *J. Chem. Neuroanat.* 11:99–111.

Perez-Clausell, J., and G. Danscher. 1986. Intravesicular localization of zinc in rat telencephalic boutons. A histochemical study. *Brain Res.* 337:91–98.

Slomianka, L. 1992. Neurons of origin of zinc-containing pathways and the distribution of zinc-containing boutons in the hippocampal region of the rat. *Neuroscience.* 48:325–352.

Spires, S., and T. Begenisich. 1992. Chemical properties of the divalent cation binding site on potassium channels. *J. Gen. Physiol.* 100: 181–193.

Spires, S., and T. Begenisich. 1994. Modulation of potassium channel gating by external divalent cations. *J. Gen. Physiol.* 104:675–692.

Talukder, G., and N. L. Harrison. 1995. On the mechanism of modulation of transient outward current in cultured rat hippocampal neurons by di- and trivalent cations. *J. Neurophysiol.* 73:73–79.

Vallee, B. L., and D. S. Auld. 1990. Zinc coordination, function, and structure of zinc enzymes and other proteins. *Biochemistry.* 29: 5647–5659.

Williams, R. J. P. 1989. An introduction to the biochemistry of zinc. *In* Zinc in Human Biology. C. F. Mills, editor. Springer-Verlag, Berlin. 15–31.

Wooltorton, J. R. A., and A. Mathie. 1993. Block of potassium currents in rat isolated sympathetic neurons by tricyclic antidepressants and structurally related compounds. *Br. J. Pharmacol.* 110:1126–1132.

Yang, J., P. T. Ellinor, W. A. Sather, J. F. Zhang, and R. W. Tsien 1993. Molecular determinants of $Ca^{2+}$ selectivity and ion permeation in L-type $Ca^{2+}$ channels. *Nature.* 366:158–161.